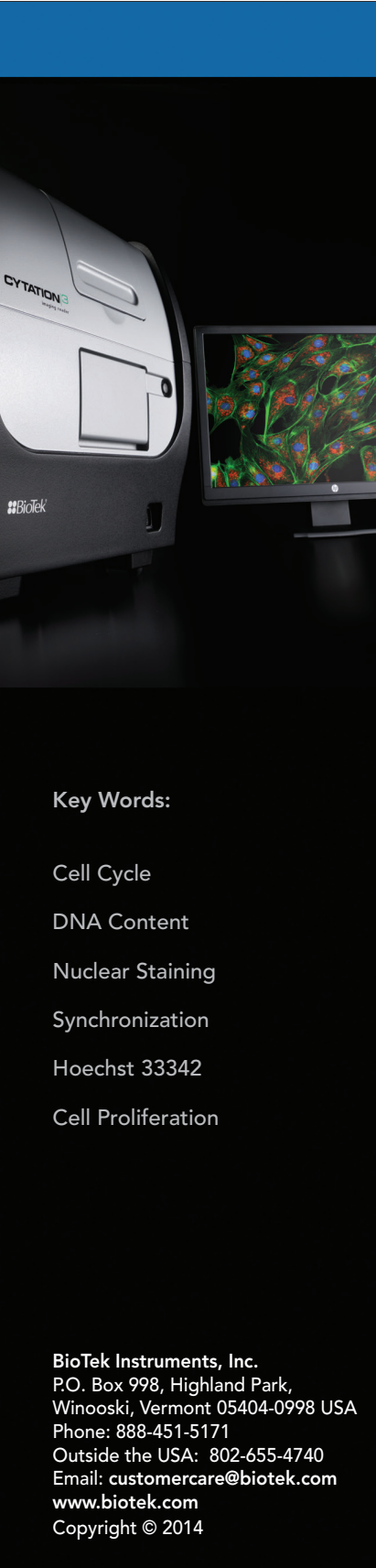


Cell Synchrony Determination Using Microscopic Imaging

Use of Nuclear Staining to Assess Cell Cycle Stage by Nuclear DNA Content

Paul Held Ph. D., Laboratory Manager, Applications Department, BioTek Instruments, Inc., Winooski, VT



The effect of compounds on cellular proliferation is a key element of the ADME/Tox drug discovery process. With any anti-cancer chemotherapy it is necessary to determine not only the relative toxicity of the agent in normal and tumor cells, but also any effects these agents have on cell cycle progression. Here we describe the use of nuclear staining dyes in conjunction with image based analysis to assess the effects of compounds on cell cycle progression in adherent cells.

Introduction

The replication of cells is responsible for tissue, organ, and species growth and reproduction. Although an increase in cell mass may play a role in growth, proliferation - an increase in the number of cells - is by far more important. Proliferating cells repeatedly transition between cellular duplication or interphase and cell division or mitosis. The concept of cell cycle was first utilized to describe these repetitive elements. The terminology (G_0 , G_1 , S, G_2 , and M) attempts to place in temporal perspective two dichotomies; mitosis (M), which can be determined by direct observation, and DNA synthesis (S), which can be established by DNA labeling. G_1 , the post mitotic gap, G_2 the post-synthetic phase or pre-mitotic gap; and G_0 , a phase in which non-dividing cells exist, are terms used for simplicity (Figure 1).

This basis of cell cycle analysis was first described using Feulgen staining for flow cytometry [1] and later modified to use propidium iodide [2]. Resting cells (G_0/G_1 phase) contain two copies of each chromosome. As cells progress toward mitosis, they synthesize DNA (S phase), allowing more stain intercalation with an accompanying increase in fluorescence intensity. When all chromosomes have replicated and the DNA content has doubled (G_2/M phase), the cells fluoresce with twice the intensity of the G_0/G_1 population. The G_2/M cells eventually divide into two cells with the DNA equally distributed between the daughters, thus halving the intensity of the nuclear stain. Using these methods, care must be made to insure that cell doublets are excluded, as two G_0/G_1 cells have the same nuclear content as a single G_2 cell.

Other nucleic acid stains have been used for imaging, including, DAPI [3], Hoechst 33342 [4], and DRAQ5 [5], the latter two having the advantage of being cell membrane permeable allowing their use with live cells.

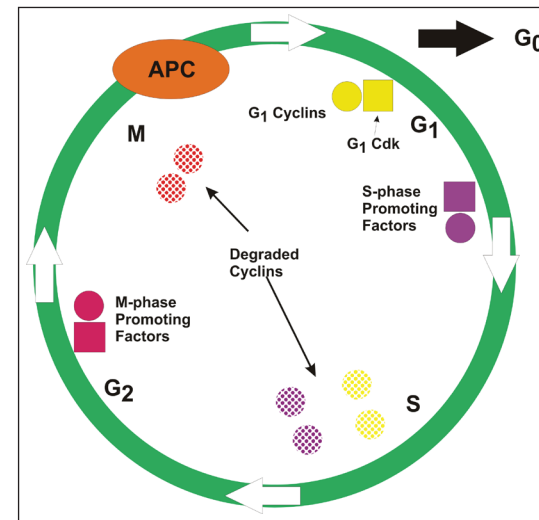


Figure 1. Schematic of Cell Cycle.

Progression through the cell cycle is a highly regulated process with a number of checkpoints. Two classes of regulatory molecules, cyclins and cyclin-dependant kinases (Cdks) are responsible for cell cycle progression control (Figure 1). These genetically conserved proteins work in concert as heterodimers with the cyclins serving as regulators, while Cdks serve as the catalytic units.

Cyclins have no catalytic activity and Cdk's are inactive in the absence of a partner cyclin. When activated by a bound cyclin, Cdk's phosphorylate specific proteins resulting in their activation or inactivation depending on the protein.

The protein target is dependent on the combination of cyclin and Cdk. Cdk's are constitutively expressed in cells whereas cyclins are synthesized at specific stages of the cell cycle, in response to various molecular signals [6].

The compounds used in these studies have all been previously shown to stall cells in various stages of the cell cycle or at higher doses, become cytotoxic. Vinblastine, a vinca alkaloid used in the treatment of several cancers, inhibits microtubule formation by disrupting microtubule dynamic behavior [7-8]. Likewise, nocodazole works to prevent microtubule polymerization [9]. With exposure to either compound, cells cannot undergo mitosis, despite duplicating their DNA, and cellular nuclear content remains at G₂ levels. The nucleoside thymidine in high levels is known to result in a negative feedback on the production of deoxycytidine triphosphate without which DNA cannot be replicated and cells stall in S-phase [10]. Because the cellular feedback loop is not absolute, after an initial exposure to thymidine cells are released and then blocked with a second round of drug in a process known as double thymidine block in order to improve cell synchronization [11]. Hydroxyurea inactivates the enzyme ribonucleotide reductase, a key component in DNA replication, which also stalls cells in S-phase [12-13].

Materials and Methods

NIH3T3, and HeLa cells were grown in Advanced DMEM (cat # 12491) from Life Technologies supplemented with 10% FBS, 2 mM glutamine. Black-sided, clear bottom 96-well microplates (cat# 3603) were from Corning. TopSeal-A (cat # 6050195) adhesive plate sealers were from PerkinElmer. DAPI dihydrochloride stain (cat# D1306), Hoechst 33342 (cat# H1399) and DPBS (cat# 14190), were obtained from Life Technologies.

Drug Treatment

Cells were trypsinized from stock cultures and seeded into 96-well microplates at a concentration of 5000 cells per well in a volume of 100 μ L and allowed to attach overnight (16 hrs). The following day the intended drug treatment was added in 100 μ L as a 2x stock diluted in full media. Cells were exposed to drug treatment for 24 hours then stained with Hoechst 33342 prior to imaging.

Cell Staining

Cell nuclei were then stained with 50 μ L of (5x) working solution of Hoechst 33342 added directly to the 200 μ L of media in the microplate for a final concentration of 30 μ M. Working solution (5x) was prepared from a 14.3 mM stock by dilution to 150 μ M in full cell media. Cells were stained 15 minutes at 37°C 5% CO₂ immediately prior to imaging.

Cell Imaging

Cells were imaged using a Cytaion™ 3 Cell Imaging Multi-Mode Reader (BioTek Instruments, Winooski, VT) configured with DAPI, GFP and Texas Red light cubes. The imager uses a combination of LED light sources in conjunction with band pass filters and dichroic mirrors to provide appropriate wavelength light. The DAPI light cube is configured with a 377/50 excitation filter and a 447/60 emission filter; the GFP light cube uses a 469/35 excitation filter and a 525/39 emission filter; while the Texas Red light cube uses a 586/15 excitation and 647/57 emission filters.

All cell counting experiments were performed using a 4x microscope objective; while visualization of DNA staining of nuclei was performed using a 20x microscope objective.

Image Analysis

Cell object counting analysis was performed on the DAPI channel data for all experiments. Initial object threshold was set to 10,000 with a minimum object size of 5 μ M and a maximum size set to 100 μ M. Background was evaluated on the 5% lowest pixels, image smoothing was set to 3 cycles, background flattening size was set to auto, and touching objects were split. Cut off values for G₁, S and G₂/M phase were set empirically based on object data obtained from untreated control wells.

Histogram Analysis

After cellular analysis individual object data was exported to Microsoft Excel. Frequency histograms of object DAPI signal mean signals were generated. Frequency bin of equal size were generated by parsing the minimum and maximal signal into 100 segments. Care was taken to identify and eliminate high intensity objects, often multiple cells, designated as a single entity by the software.

Results

Treatment of cells by compounds can result in cells being halted at various points of the cell cycle. With nuclear staining cells can be identified as being in G₁ or G₂/M based on the intensity of nuclear fluorescence. As demonstrated in Figure 2, vinblastine treatment can result in an enrichment of cells in G₂/M and those nuclei can be differentiated from nuclei with G₁ content.

The treatment of cells with Nocodazole is known to halt progression of the cell cycle in G₂ phase [6]. Because G₂ cells have 2x the nuclear content of G₁ cells they can be identified through threshold analysis of Hoechst 33342 staining. As demonstrated in Figure 3, exposure to increasing concentrations of Nocodazole results in a greater percentage of cells having a 2x nuclear content as measured by nuclear staining intensity. At high concentrations approximately 80% of the cells have 2x nuclear content, whereas low concentration and untreated cells have approximately 15%.

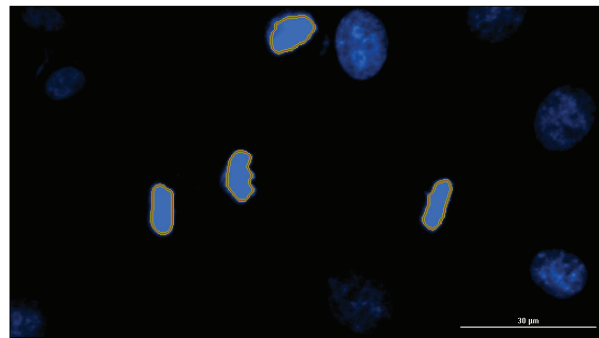


Figure 2. Hoechst 33342 stained HeLa cell nuclei. Vinblastine treated cells were stained with Hoechst 33342 and G₂/M content nuclei identified (yellow trace) with object cellular analysis.

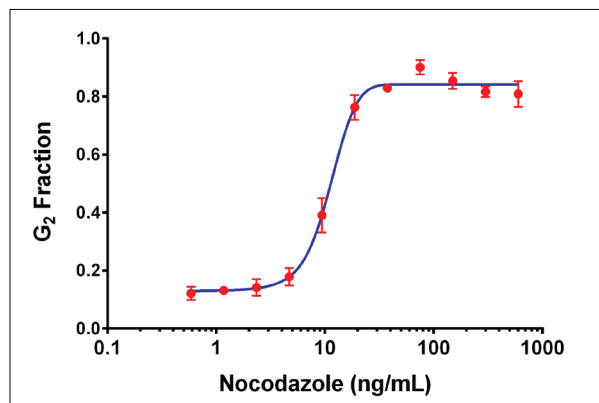


Figure 3. Nocodazole treatment of HeLa cells.

Conversely, hydroxyurea, which halts cells in S-phase [7] can be shown to reduce the fraction of G₂ cells in NIH3T3 cells in a concentration dependant manner. Untreated NIH3T3 cells have approximately 15% of their numbers in G₂ phase of the cell cycle. With increasing concentrations of hydroxyurea this percentage falls to about 1% after a 24 hours exposure (Figure 4).

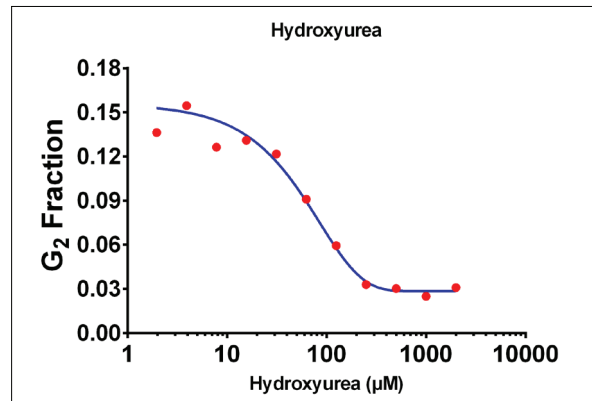


Figure 4. Hydroxyurea treatment of NIH3T3 cells.

Vinblastine treatment of cultured cells has also been shown to stall cells in G₂ phase of the cell cycle [8]. With increasing concentrations of vinblastine the percentage of cells identified as G₂/M by nuclear staining increases 3-fold, while cells identified as having G₁ content decreases accordingly (Figure 5).

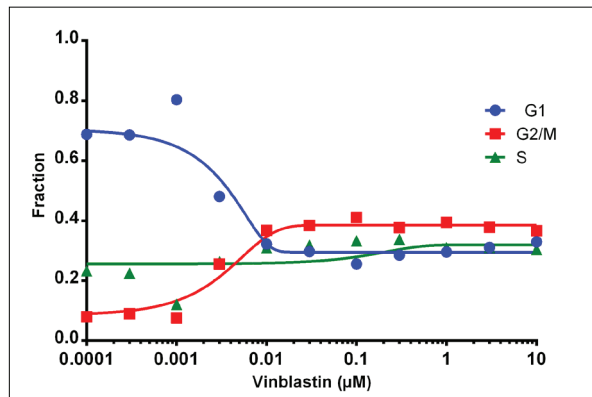


Figure 5. Vinblastine treatment of HeLa cells.

Cellular nuclear content can also be assessed using frequency histograms of fluorescence intensity. When cellular nuclei are identified using object counting image analysis, a number of different individual object parameters are also available for further analysis. For example, the individual object mean fluorescence intensity measurements can be plotted as frequency histograms, which is an analysis often used when nuclear content is assessed with flow cytometry.

As shown in Figure 6, untreated asynchronous HeLa cells grown in 10% serum demonstrate a major frequency peak that corresponds to cells with G₁ nuclear content, as well as a smaller less well defined peak that corresponds to G₂. The intermediate region of nuclear content between G₁ and G₂ cells represents cells in S-phase undergoing the process of duplication their DNA. Cells treated with thymidine demonstrate a build-up of cells stalled in S phase.

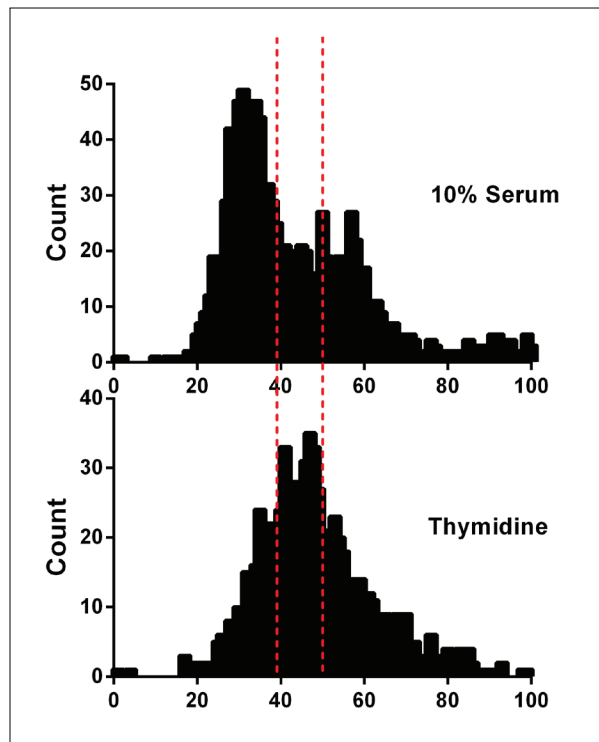


Figure 6. Nuclear content of thymidine and untreated HeLa cells. Histogram of control cells (10% serum) with no treatment show a two peak distribution from a heterogeneous population of G₁-phase and G₂/M-phase. Histogram of thymidine (2 mM) treated cells shows a shift in the distribution of a population of cells, predominately in the S-phase of cell cycle. Dashed lines indicate fluorescence intensity of S-phase nuclear content.

Discussion

The effect of drug compounds on the cell cycle is a closely monitored effect during the early stages of drug development. Historically these studies were performed with fluorescent stained cells using flow cytometry, which has limited throughput capabilities [14]. These data demonstrate that image analysis using stained cells in microplates is a useful and viable alternative that allows greater sample throughput.

In this treatise, live cells were stained and imaged without fixation. Besides saving time, live cell imaging offers some advantages over fixed and stained cell imaging.

Foremost is the fact that live cell imaging can provide data regarding cellular processes over time. While fixed and stained cells can be probed with an almost limitless number of antibodies, this technique is static and offers only a one-time snapshot in time as to what is occurring. Additionally, the live stained cells are available for other types of analysis after nuclear content determination.

Cytation 3 is an ideal platform for live cell imaging. The capability of having up to four different colors and two objectives allows both rapid screening and detailed high magnification imaging of stained cells. In addition to its imaging features, the Cytation 3 offers a full complement of top-read microplate reader capabilities including dual monochromator and filter based fluorescence detection. The reader can be configured with the BioTek Gas Controller module, which allows for control of carbon dioxide and oxygen levels in the read chamber. This allows the researcher to run long term kinetic measurements on microplates unattended without the worry of maintaining media pH. In addition, the reader can be configured with dual injectors, which allow for the addition of cellular dyes in mid run, shortly before imaging; thus reducing exposure time to the dye, while still providing the ability to run long-term experiments unattended.

References

1. Van Dilla, M. A., T. T. Truiullo, P. F. Mullaney, J.R. Coulter (1969) Cell Microfluorometry: A Method for Rapid Fluorescence Measurement, *Science* 163:1213-1214 DOI: 10.1126.
2. Krishan A. (1975) [Rapid flow cytofluorometric analysis of mammalian cell cycle by propidium iodide staining](#). *J. Cell Biology* 66 (1):188-193.
3. Kapuscinski J (September 1995). "DAPI: a DNA-specific fluorescent probe". *Biotech Histochem* 70 (5): 220-33. PMID 8580206.
4. Portugal, J; Waring, MJ (Feb 28, 1988). "Assignment of DNA binding sites for 4',6-diamidino-2-phenylindole and bisbenzimide (Hoechst 33258). A comparative footprinting study". *Biochimica et Biophysica Acta* 949 (2): 158–68. doi:10.1016/0167-4781(88)90079-6. PMID 2449244
5. Smith, P.J., Wiltshire, M., Davies, S., Patterson, L.H., Hoy, T. (1999) [A novel cell permeant and far red-fluorescing DNA probe, DRAQ5, for blood cell discrimination by flow cytometry](#). *J. Immunol. Methods*, 229:131-139.

6. Vermeulen, K. D.R. Van Bockstaele, and Z.N. Berneman (2003) The Cell Cycle: a Review of Regulation, Deregulation and Therapeutic Targets in Cancer, *Cell Prolif.* 36:131-149.

7. Tashiro, E., S. Simizu, M. Takada, K. Umezawa, and M. Imoto (1998) Caspase-3 Activation is Not Responsible for Vinblastin-induced Bcl-2 Phosphorylation and G2/M Arrest in Human Small Lung Carcinoma Ms-1 Cells, *Jpn. J. Cancer Res.* 89:940-946.

8. Dhamodharan, R., M.A. Jordan, D. Thrower, L. Wilson, and P. Wadsworth (1995) Vinblastine Suppresses Dynamics of Individual Microtubules in Living Interphase Cells, *Mol. Biol. Of the Cell*, 6:1215-1229. PMCID: PMC301278.

9. Vasquez, R.J. B. Howell, A.M. Yvon, P. Wadsworth, and L. Cassimeris (1997) Nanomolar Concentrations of Nocodazole alter Microtubule Dynamic Instability in vivo and in vitro, *Mol Biol. Cell* 8(6):973-985. PMCID: PMC305707

10. Xeros, N. (1962) Deoxyriboside Control and Synchronization of Mitosis, *Nature*, 194:682-683.

11. Bostock, C.J., D.M. Prescott, and J.B. Kirkpatrick (1971) An Evaluation of the Double Thymidine Block for Synchronizing Mammalian Cells at the G1-S Border, *Exp. Cell Res.* 68(1):163-168.

12. Yarbro, J.W. (1992) Mechanism of Action of Hydroxyurea, *Semin. Oncol.* 19(3): 1-10. PMID:1641648

13. Adams, R.L.P. and J.G. Lindsay (1967) Hydroxyurea Reversal of Inhibition and use as a Cell-Synchronizing Agent. *J. Biol. Chem.* 242(6):1314-1317.

14. Merrill, G.F. (1998) Cell Synchronization, Methods *Cell. Biol.* 57:229-249.

RA44419.424212963

5994-3348EN
September 1, 2021